Monthly Notices of the ROYAL ASTRONOMICAL SOCIETY

MNRAS **514,** 3017–3023 (2022) https://doi.org/10.1093/mnras/stac1522
Advance Access publication 2022 June 2

Host galaxy magnitude of OJ 287 from its colours at minimum light

Mauri J. Valtonen,[1,2★] Lankeswar Dey ,[3★] S. Zola ,[4,5] S. Ciprini,[6,7] M. Kidger,[8] T. Pursimo,[9] A. Gopakumar,[3] K. Matsumoto,[10] K. Sadakane,[10] D. B. Caton,[11] K. Nilsson,[1] S. Komossa,[12] M. Bagaglia,[13] A. Baransky,[14] P. Boumis ,[15] D. Boyd,[16] A. J. Castro-Tirado,[17] B. Debski,[4] M. Drozdz,[5] A. Escartin Pérez,[18] M. Fiorucci,[13] F. Garcia,[19] K. Gazeas ,[20] S. Ghosh,[3] V. Godunova,[21] J. L. Gomez,[17] R. Gredel,[22] D. Grupe,[23] J. B. Haislip,[24] T. Henning,[22] G. Hurst,[25] J. Janík,[26] V. V. Kouprianov,[24] H. Lehto,[2] A. Liakos ,[15] S. Mathur,[27,28] M. Mugrauer,[29] R. Naves Nogues,[30] G. Nucciarelli,[13] W. Ogloza,[5] D. K. Ojha,[3] U. Pajdosz-Śmierciak,[4] S. Pascolini,[13] G. Poyner,[31] D. E. Reichart,[24] N. Rizzi,[13] F. Roncella,[13] D. K. Sahu,[32] A. Sillanpää,[2] A. Simon,[33] M. Siwak,[5,34] F. C. Soldán Alfaro,[35,36] E. Sonbas,[37,38] G. Tosti,[13] V. Vasylenko,[33] J. R. Webb[39] and P. Zielinski[40]

Affiliations are listed at the end of the paper

Accepted 2022 May 30. Received 2022 May 8; in original form 2022 January 19

ABSTRACT

OJ 287 is a BL Lacertae type quasar in which the active galactic nucleus (AGN) outshines the host galaxy by an order of magnitude. The only exception to this may be at minimum light when the AGN activity is so low that the host galaxy may make quite a considerable contribution to the photometric intensity of the source. Such a dip or a fade in the intensity of OJ 287 occurred in 2017 November, when its brightness was about 1.75 mag lower than the recent mean level. We compare the observations of this fade with similar fades in OJ 287 observed earlier in 1989, 1999, and 2010. It appears that there is a relatively strong reddening of the $B - V$ colours of OJ 287 when its V-band brightness drops below magnitude 17. Similar changes are also seen in $V - R$, $V - I$, and $R - I$ colours during these deep fades. These data support the conclusion that the total magnitude of the host galaxy is $V = 18.0 \pm 0.3$, corresponding to $M_K = -26.5 \pm 0.3$ in the K-band. This is in agreement with the results, obtained using the integrated surface brightness method, from recent surface photometry of the host. These results should encourage us to use the colour separation method also in other host galaxies with strongly variable AGN. In the case of OJ 287, both the host galaxy and its central black hole are among the biggest known, and its position in the black hole mass–galaxy mass diagram lies close to the mean correlation.

Key words: galaxies: active – BL Lacertae objects: general – BL Lacertae objects: individual: OJ 287 – galaxies: bulges.

1 INTRODUCTION

OJ 287 is a BL Lacertae type quasar (RA: 08:54:48.87, Dec.: +20:06:30.6), situated at a redshift of $z = 0.306$. Based on the faintness of its optical Balmer lines from the broad-line region (Sitko & Junkkarinen 1985; Nilsson, Takalo & Lehto Sillanpää 2010), OJ 287 is classified as a BL Lac object. Given its spectral energy distribution (SED), it is of LBL type (Padovani & Giommi 1995). Optical emission lines from the narrow-line region like [O III]λ5007 are only faintly present (Nilsson et al. 2010). It shows high brightness activity at about 12 yr intervals, most likely due to a binary black hole (BH) central engine having that orbital period (Sillanpää et al. 1988; Dey et al. 2019). The binary model consists of two BHs orbiting each other in an orbit of eccentricity ∼0.65 and semimajor axis ∼0.05 pc (Dey et al. 2018). The components are unequal: the mass ratio is ∼120. The secondary cycle of activity with ∼56-yr period is also well established and it is understood as the precession cycle of the binary (Valtonen et al. 2010).

It is less well known that OJ 287 also shows prominent low-activity states called fades, at similar intervals (Takalo et al. 1990; Pietilä et al. 1999). First such prominent dip in the brightness of OJ 287 was noticed during 1989. Takalo et al. (1990) carried out a detailed study of the 1989 fade and concluded that at the minimum light, the host galaxy radiated at least the same amount of energy as the synchrotron source in the V-band. The evidence for seeing the host galaxy comes in the colours of the object: while the object's brightness fades, its SED changes from the usual power-law spectrum in the optical region to the spectrum typical of an elliptical galaxy at the redshift of $z = 0.3$ of OJ 287. In Fig. 1, we show the multicolour data of OJ 287 during the 1989 fade.

Lehto & Valtonen (1996) predicted that the fade should be repeated in 1998, one binary orbital cycle later, when the underlying binary BH system is at the same orbital phase as in 1989. Due to a strong forward precession of the major axis of the orbit, the orbital phase covers the whole cycle in less than 12 yr. The predicted fade indeed

★ E-mail: mvaltonen2001@yahoo.com (MJV); lanky441@gmail.com (LD)

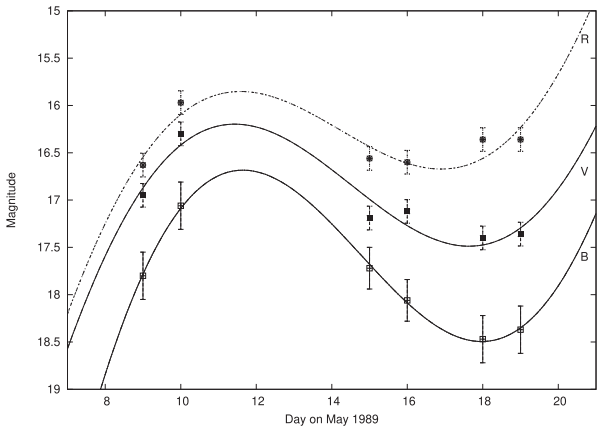

Figure 1. The observations of the 1989 fade of OJ 287 with the *Nordic Optical Telescope* and the *Jacobus Kapteyn Telescope* at La Palma, with 2σ error bars. Here, we plot the magnitudes in three filters B, V, and R. The lines are fifth-order polynomial fits through the data points.

took place, only 6 weeks after the predicted time (Pietilä et al. 1999). Since then, there have been prominent fades in 1999 and 2010, while the most recent one took place in November 2017.

In this paper, we collect the data from the fades since 1989 and compare them with the Takalo et al. (1990) data. We make use of these deepest fades to try to detect the underlying host galaxy. The host has been difficult to detect because the radiation from the active galactic nucleus (AGN) is strongly beamed towards us. During a fade, we have the best opportunity to see the host galaxy. Further, it is important to determine the host brightness in order to get another point at the upper end of the BH mass versus host bulge stellar mass diagram, where the data are few (Saglia et al. 2016).

The organization of the paper is as follows. In Section 2, we describe the photometric observations of different fades of OJ 287 used in this paper. Section 3 uses these and earlier photometric observations to calculate the changes of colour of OJ 287 as a function of its magnitude. The changes are modelled by a combination of light from the AGN and the host galaxy. In this way, the two contributions are separated, and the host magnitude is derived. In Section 4, we compare this determination of the host magnitude with the integrated surface photometry method, and find good agreement with a recent K-band determination of the host magnitude.

2 OBSERVATIONS

In anticipation of the big flare in OJ 287 in 2015 December, an observational campaign was set-up (Valtonen et al. 2016). After the detection of the flare which peaked on December 5, we continued to monitor the blazar in the wide-band R filter with the Skynet Robotic Network telescopes and at sites in Japan, Greece, Ukraine, UK, Spain, and Poland. We achieved a daily cadence except for the periods when OJ 287 was too close to the sun or the moon. On several occasions, we also took multifilter data. All photometric observations were reduced by a single person (S.Z.) to provide as uniform as possible data set. The reduction is done in a standard way: images were calibrated for bias, dark and flat-field and we extracted magnitudes using the aperture method. More details about the procedure were given in Pihajoki et al. (2013).

The left-hand panel of Fig. 2 shows OJ 287 observations which we gathered during the 2017/18 season. In the right-hand panel of Fig. 2, we present how this recent fade compares with earlier ones. We note that the minimum light at 2017.85 is 1.75 mag below the oscillating historical average shown by the dotted line (oscillation period is ∼56 yr; Valtonen et al. 2006).

Older data were obtained from Perugia for the 1998–1999 fade and are presented in Table 1 (for details, see Massaro et al. 2003; Ciprini et al. 2008). The data for more recent 2006, 2010 and 2017 fades are given in Table 2. In addition to professional observatories, several amateur astronomers also contributed to the data. Some of these fades happen about six months after the time when the secondary is close to the jet line (expected jet-line minima at 1988.95 and 1997.61 in the binary central engine model; Valtonen et al. 2022), while others do not have such a connection to the orbit. The latest 'jet-line' fade was expected around 2020.53, at the time when OJ 287 was not observable by ground-based optical telescopes (Valtonen et al. 2022).

3 COLOURS OF OJ 287 AND ITS HOST

In this section, we compare colours of OJ 287 at various V-magnitude levels with those corresponding to a hypothetical host galaxy. For a supergiant elliptical galaxy at the redshift of 0.3, the expected colours are: $B-V=1.43\pm0.1$, $V-R=0.91\pm0.05$, $V-I=1.56\pm0.1$, and $R-I=0.65\pm0.05$, for a passive evolutionary model (Kristian, Sandage & Westphal 1978; Bruzual 1983; Guiderdoni & Rocca-Volmerange 1987, 1988; Fioc & Rocca-Volmerange 1997).

For OJ 287, in addition to the steady light from the host, there is a highly variable radiation from the AGN. The AGN component radiates synchrotron radiation with a constant spectral index $\alpha\sim1.5$ (the flux $F_\nu\sim\nu^{-\alpha}$) over the V-magnitude range from 16.5 to 14, irrespective of the flux level (Kidger et al. 1995; Hagen-Thorn et al. 1998). The only confirmed exception to this rule arises during the thermal flares when the flux rise makes $V\leq13.5$ and the spectrum becomes exceptionally blue (Valtonen, Ciprini & Lehto 2012; Valtonen et al. 2016). The second possible exception, discussed in this paper, occurs when brightness in V drops below about 17 mag. Aside from those special episodes, the colours of OJ 287 are: $B-V=0.57\pm0.13$, $V-R=0.44\pm0.09$, and $V-I=1.11\pm0.16$ (Efimov et al. 2002).

In order to model the gradual change of colours due to an underlying galaxy, we first carried out a second-order polynomial fit to all the available colours as a function of magnitude. The $B-V$, $V-R$, $V-I$, and $R-I$ colours were taken from the values shown in Tables 1 and 2 as well as from the previously published values in Takalo et al. (1990). One such fit is shown in Fig. 3 for example, where we plot the $B-V$ at different V intervals of OJ 287 and the red dash–dotted line shows the polynomial fit. The expected colours of the host galaxy and the AGN are marked by the horizontal lines in these graphs (see Fig. 3). There is an upward curvature of the best fit which is significant above 3σ level in all except in the $R-I$ diagram. We identified the possible location of the host in the magnitude axis as the point where the fit to the observations meets the host line. At this brightness, practically all the light comes from the host galaxy.

Determined in this way, we find that the host galaxy magnitude is $V=18.2\pm0.3$ from the $B-V$ data, $V=17.5\pm0.5$ from the $V-R$ data, and $V=17.25\pm0.5$ from the $V-I$ data. In the $R-I$ diagram, the AGN and host galaxy lines are so close to each other that we cannot derive the host magnitude. The standard deviation of the fit through points is included in the error estimate. Also the error limit includes the error in the expected colour of the host as mentioned above.

Simulations of the colours derived from the optical spectrum (power law plus host galaxy model) in different states can be used to evaluate the effective capability of the method. With this method,

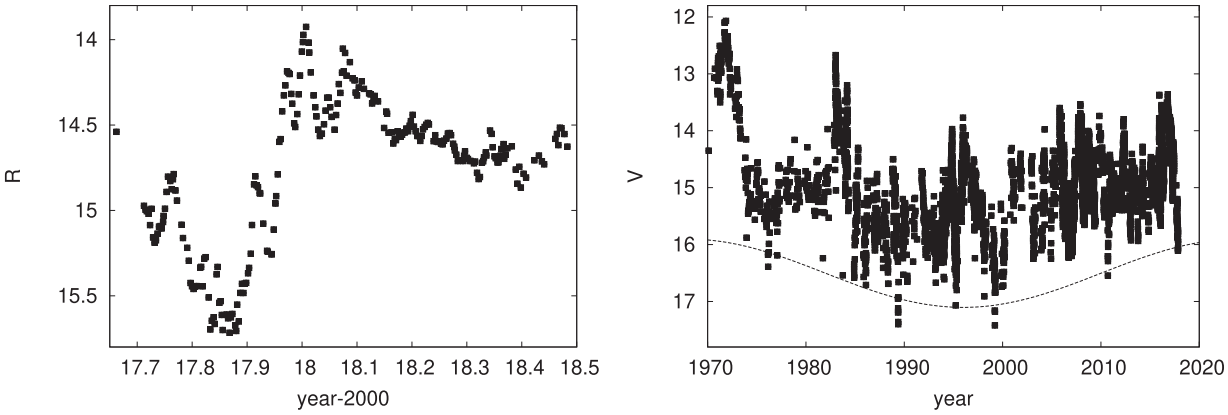

Figure 2. Left-hand panel: The *R*-band optical light curve of OJ 287 in the 2017/18 season. Right-hand panel: The *V*-band optical light curve of OJ 287 from 1970 to 2018. The dotted line runs 1.75 mag below the historical mean brightness of OJ 287.

Table 1. Perugia VRI observations of the 1998 and 1999 fades.

Year	*V*	*R*	*I*	Year	*V*	*R*	*I*
1998.0218	16.08 ± 0.11	15.26 ± 0.05	14.56 ± 0.03	1998.9614	16.35 ± 0.19	15.85 ± 0.07	15.15 ± 0.05
1998.0223	16.09 ± 0.09	15.57 ± 0.06	14.71 ± 0.04	1998.9616	–	15.71 ± 0.07	15.10 ± 0.064
1998.1312	16.40 ± 0.13	16.09 ± 0.08	14.96 ± 0.04	1998.9637	15.83 ± 0.18	15.89 ± 0.06	15.10 ± 0.045
1998.1338	15.92 ± 0.06	15.72 ± 0.04	15.27 ± 0.04	1998.9642	–	15.68 ± 0.06	15.17 ± 0.05
1998.1366	16.91 ± 0.13	16.01 ± 0.06	15.10 ± 0.04	1998.9748	–	15.77 ± 0.05	14.95 ± 0.04
1998.1394	16.53 ± 0.13	16.34 ± 0.10	15.01 ± 0.04	1999.0128	16.26 ± 0.23	15.51 ± 0.05	14.87 ± 0.04
1998.1421	–	15.69 ± 0.07	15.08 ± 0.04	1999.0134	–	15.68 ± 0.06	14.83 ± 0.04
1998.1559	16.78 ± 0.14	15.79 ± 0.06	15.15 ± 0.04	1999.0136	–	15.63 ± 0.06	14.86 ± 0.04
1998.1586	16.63 ± 0.12	15.67 ± 0.05	15.17 ± 0.04	1999.0157	15.88 ± 0.19	15.67 ± 0.05	15.07 ± 0.04
1998.1668	16.41 ± 0.20	15.61 ± 0.08	15.00 ± 0.05	1999.0164	–	15.76 ± 0.13	14.92 ± 0.08
1998.1695	15.94 ± 0.10	15.59 ± 0.06	15.03 ± 0.05	1999.0239	–	15.92 ± 0.07	15.02 ± 0.04
1998.1777	15.96 ± 0.06	15.40 ± 0.05	–	1999.0951	–	15.67 ± 0.09	15.25 ± 0.08
1998.1887	–	15.57 ± 0.06	14.86 ± 0.04	1999.1058	–	15.82 ± 0.07	15.07 ± 0.05
1998.1996	16.30 ± 0.11	15.78 ± 0.06	14.96 ± 0.04	1999.1196	–	15.44 ± 0.06	14.78 ± 0.04
1998.2049	15.72 ± 0.10	15.47 ± 0.06	14.48 ± 0.04	1999.1524	–	16.00 ± 0.07	15.34 ± 0.05
1998.2103	15.82 ± 0.08	15.33 ± 0.05	14.75 ± 0.04	1999.1551	–	15.53 ± 0.06	15.09 ± 0.05
1998.2158	–	15.40 ± 0.12	14.76 ± 0.10	1999.1688	–	16.13 ± 0.12	15.56 ± 0.07
1998.2350	–	15.48 ± 0.05	14.85 ± 0.04	1999.1825	–	16.19 ± 0.10	15.56 ± 0.06
1998.2377	16.51 ± 0.16	15.63 ± 0.06	14.92 ± 0.05	1999.1880	–	16.22 ± 0.22	15.80 ± 0.16
1998.2405	16.35 ± 0.21	15.82 ± 0.08	–	1999.1907	–	16.23 ± 0.09	15.68 ± 0.07
1998.2432	16.07 ± 0.20	–	14.90 ± 0.05	1999.1934	–	16.02 ± 0.08	15.41 ± 0.06
1998.2461	16.05 ± 0.19	15.65 ± 0.13	14.81 ± 0.07	1999.1961	–	15.88 ± 0.08	15.16 ± 0.05
1998.2541	15.90 ± 0.11	15.41 ± 0.06	14.77 ± 0.05	1999.2016	–	16.02 ± 0.07	15.62 ± 0.06
1998.2568	16.01 ± 0.16	15.45 ± 0.06	14.59 ± 0.04	1999.2044	–	16.12 ± 0.11	15.37 ± 0.06
1998.2705	15.79 ± 0.09	15.44 ± 0.05	14.84 ± 0.04	1999.2153	–	17.02 ± 0.18	15.85 ± 0.10
1998.3006	15.96 ± 0.08	15.29 ± 0.05	–	1999.2155	–	16.31 ± 0.10	15.69 ± 0.07
1998.3034	16.00 ± 0.09	15.41 ± 0.05	14.75 ± 0.04	1999.2180	–	15.94 ± 0.08	15.44 ± 0.06
1998.3061	15.89 ± 0.13	15.24 ± 0.05	14.78 ± 0.05	1999.2235	–	16.78 ± 0.15	15.95 ± 0.08
1998.3089	15.86 ± 0.09	15.42 ± 0.07	14.74 ± 0.04	1999.2453	–	16.34 ± 0.15	16.09 ± 0.11
1998.3144	15.39 ± 0.09	15.24 ± 0.07	14.72 ± 0.05	1999.2508	–	16.24 ± 0.12	15.73 ± 0.09
1998.3171	–	15.20 ± 0.09	14.58 ± 0.06	1999.2562	–	16.21 ± 0.11	15.94 ± 0.09
1998.9583	16.89 ± 0.38	16.01 ± 0.09	14.85 ± 0.04	1999.2727	–	16.44 ± 0.11	15.84 ± 0.08
1998.9610	–	15.76 ± 0.05	15.07 ± 0.04				

we calculate the theoretical line more accurately. We add the AGN of the above-mentioned colour to a host of a given *V*-magnitude. Different host magnitudes were applied until we find one which gives a good fit to the observations. The result is shown by the black dashed line in Fig. 3. The calculations are carried out in linear flux units, and subsequently converted to magnitudes. The scatter in the observational points is similar to earlier studies (Efimov et al. 2002).

From Fig. 3, we find that the simulation study supports the host galaxy magnitude to be $V = 18.0 \pm 0.3$. However, the faintest *R*-band value, 17.0 ± 0.2 (observed in Perugia in 1999), puts an upper limit to the host brightness of $V \sim 17.7$. All data are thus consistent with $V = 18.0 \pm 0.3$.

Note that the 2017 high-accuracy observations from Krakow and Mt. Suhora Observatories as well as the UK and Spanish observations, even though with a larger scatter, agree perfectly with the expected colour behaviour that arises from adding the host and the AGN components. This would be very surprising if the underlying reason for the colour changes is something else than the influence

Table 2. Krakow and Mt. Suhora BVRI observations of the 2006, 2010, and 2017 fades.

Year	*B*	*V*	*R*	*I*
2006.7400	–	15.85 ± 0.03	15.42 ± 0.02	14.77 ± 0.01
2006.7455	–	15.72 ± 0.02	15.30 ± 0.02	14.66 ± 0.01
2006.7482	–	15.64 ± 0.01	15.21 ± 0.01	14.56 ± 0.01
2006.7647	–	15.54 ± 0.02	15.11 ± 0.01	14.46 ± 0.01
2006.7730	–	15.44 ± 0.01	15.01 ± 0.01	14.36 ± 0.01
2006.7756	–	15.60 ± 0.01	15.15 ± 0.01	14.50 ± 0.01
2006.7757	–	–	15.12 ± 0.03	14.43 ± 0.02
2006.7783	–	–	15.09 ± 0.01	14.45 ± 0.02
2006.7921	–	15.85 ± 0.02	15.40 ± 0.01	14.74 ± 0.02
2006.7948	–	16.01 ± 0.02	15.57 ± 0.01	14.89 ± 0.01
2006.7940	16.61 ± 0.04	16.02 ± 0.02	15.57 ± 0.01	14.85 ± 0.02
2006.7976	–	15.97 ± 0.04	15.50 ± 0.01	14.84 ± 0.02
2006.8003	–	15.68 ± 0.02	15.26 ± 0.02	14.62 ± 0.01
2006.8524	16.56 ± 0.03	16.01 ± 0.03	15.56 ± 0.02	14.92 ± 0.02
2006.8551	16.23 ± 0.08	15.60 ± 0.11	15.18 ± 0.10	14.57 ± 0.08
2006.8742	16.14 ± 0.04	15.59 ± 0.02	15.17 ± 0.02	14.54 ± 0.02
2006.8800	16.16 ± 0.03	15.59 ± 0.01	15.17 ± 0.01	14.52 ± 0.01
2006.9070	15.97 ± 0.01	15.43 ± 0.02	15.02 ± 0.01	14.38 ± 0.01
2006.9097	16.06 ± 0.01	15.49 ± 0.01	15.07 ± 0.01	14.44 ± 0.01
2006.9150	16.09 ± 0.02	15.51 ± 0.02	15.09 ± 0.02	14.44 ± 0.02
2006.9234	16.13 ± 0.05	15.56 ± 0.01	15.10 ± 0.02	14.46 ± 0.02
2006.9290	16.08 ± 0.01	15.53 ± 0.02	15.11 ± 0.03	14.47 ± 0.03
2006.9452	16.41 ± 0.03	15.82 ± 0.02	15.35 ± 0.02	14.70 ± 0.01
2006.9534	16.36 ± 0.01	15.78 ± 0.01	15.32 ± 0.01	14.65 ± 0.02
2006.9588	16.48 ± 0.01	15.88 ± 0.02	15.45 ± 0.02	14.78 ± 0.02
2006.9863	16.32 ± 0.02	15.74 ± 0.02	15.31 ± 0.01	14.65 ± 0.02
2006.9889	16.37 ± 0.01	15.80 ± 0.01	15.36 ± 0.01	14.69 ± 0.01
2006.9946	16.55 ± 0.02	15.98 ± 0.02	15.54 ± 0.01	14.88 ± 0.01
2007.0270	16.43 ± 0.04	15.85 ± 0.02	15.39 ± 0.02	14.72 ± 0.02
2007.0328	–	15.77 ± 0.06	15.33 ± 0.03	14.69 ± 0.03
2007.0386	16.62 ± 0.02	16.03 ± 0.02	15.57 ± 0.01	14.89 ± 0.02
2007.0442	16.60 ± 0.03	16.00 ± 0.02	15.55 ± 0.03	14.94 ± 0.02
2007.0708	–	16.05 ± 0.02	15.61 ± 0.03	14.96 ± 0.01
2007.1228	16.60 ± 0.01	16.04 ± 0.01	15.60 ± 0.01	14.94 ± 0.01
2007.1315	16.36 ± 0.02	15.78 ± 0.02	15.35 ± 0.01	14.71 ± 0.02
2007.1339	16.21 ± 0.05	15.66 ± 0.02	15.23 ± 0.01	14.59 ± 0.01
2007.1529	–	15.63 ± 0.01	15.18 ± 0.01	14.53 ± 0.01
2007.1750	16.19 ± 0.01	15.64 ± 0.01	15.21 ± 0.01	14.56 ± 0.02
2007.1777	16.21 ± 0.04	15.62 ± 0.03	15.20 ± 0.02	14.59 ± 0.02
2007.1802	16.30 ± 0.02	15.72 ± 0.02	15.28 ± 0.02	14.64 ± 0.02
2007.1939	16.20 ± 0.02	15.66 ± 0.01	15.22 ± 0.01	14.60 ± 0.01
2007.1967	16.16 ± 0.02	15.61 ± 0.01	15.20 ± 0.01	14.58 ± 0.01
2010.6989	–	16.23 ± 0.01	15.81 ± 0.01	15.20 ± 0.01
2010.7290	–	16.09 ± 0.03	15.64 ± 0.02	15.04 ± 0.01
2010.8059	16.01 ± 0.01	15.55 ± 0.01	15.12 ± 0.01	–
2010.8085	–	15.60 ± 0.01	15.18 ± 0.01	14.55 ± 0.01
2010.8113	–	15.63 ± 0.01	15.22 ± 0.01	14.59 ± 0.02
2010.8278	–	15.63 ± 0.01	15.20 ± 0.01	–
2011.1555	15.86 ± 0.01	–	15.03 ± 0.01	–
2017.8717	16.60 ± 0.01	16.03 ± 0.01	15.63 ± 0.01	14.99 ± 0.01
2017.9182	15.82 ± 0.01	15.26 ± 0.01	14.89 ± 0.01	14.29 ± 0.01
2018.0221	15.32 ± 0.01	14.77 ± 0.01	14.40 ± 0.01	13.82 ± 0.01

of the host. Remember that the base level of OJ 287 was about one magnitude fainter in 1989 and 1999 than in 2017. If the colour changes were related to the relative drop in brightness at the fade, then we should have seen a prominent upturn of 2017 points at higher *V* which clearly is not there.

The best spectral range for the host galaxy study is from *B* to *V*. This is because the expected host galaxy flux turns down strongly below the *V*-band wavelength while the AGN flux does not. In the $B - V$ diagram, the six points of highest *V* value come from Takalo et al. (1990). The minima according to the fits to the data happen first in the *R*-band, half-a-day later in the *V*-band, and another half-a-day later in the *B*-band. If we assume that OJ 287 has the same light-curve shape in all channels, but the light curves are shifted as mentioned, then the scatter in the points around the theoretical line is reduced. Note that the fade occurred two weeks earlier at 22 and 37 GHz radio frequencies, supporting the idea of the wavelength dependence of the timing of fades.

4 DISCUSSION AND CONCLUSIONS

There have been several attempts to measure the host galaxy magnitude by direct imaging, after subtracting the point-like AGN from the image. The task is difficult since the brightness difference between the host and the AGN is typically about 2 mag in the *K*-band, 3 mag in the *I*-band, and even greater at shorter optical wavelengths (Nilsson et al. 2020). The most favourable contrast between the AGN and the host so far has been obtained in infrared. Nilsson et al. (2020) reported recent infrared observations at the 2.5-m *Nordic Optical Telescope* when the AGN was at a low state. Imaging data were also obtained at the 10.4-m *Gran Telescopio Canarias* somewhat after the 2017 deep fade. They essentially confirm the findings of this paper, as we will discuss below.

We have determined the magnitude of the host galaxy of the BL Lacertae object OJ 287 using the change of the colour of the object during its minimum light. It is interesting to translate the result to the *K*-band for a direct comparison with the surface brightness method. Using the distance modulus $m - M = 41$, $V - K = 3.2$ (Fioc & Rocca-Volmerange 1997; Ho et al. 2011), and the combined *K*-correction and evolution correction of −0.3 in the *K*-band (Kristian, Sandage & Westphal 1978; Bruzual 1983; Guiderdoni & Rocca-Volmerange 1987, 1988; Fioc & Rocca-Volmerange 1997; Chilingarian, Melchior & Zolotukhin 2010; Nilsson et al. 2020), we obtain the absolute *K*-band magnitude of OJ 287 $M_K = -26.5 \pm 0.3$. This may be compared with the absolute *K*-band magnitude $M_K = -26.8$ of the nearby elliptical galaxy NGC 4889; the other nearby supergiant NGC 1600 is a little fainter (Thomas et al. 2016). These two galaxies are interesting as their central BH masses agree with the primary BH mass in OJ 287 within error limits (Valtonen et al. 2010).

In Fig. 4, we place OJ 287 in the BH mass versus galaxy mass diagram (Saglia et al. 2016). We see from Fig. 4 that OJ 287 is slightly, but not significantly, above the line for the mean linear correlation for nearby galaxies. If it were placed in the corresponding graph for galaxies at redshift 0.5 (Portinari et al. 2012), the result would be very much the same.

All studies of the magnitude of OJ 287 by the imaging method have been limited to the distance range 5–35 kpc from the centre. The light from the rest of the galaxy has to be extrapolated using models. Nilsson et al. (2020) find the *K*-band magnitudes, $K = 14.25$ and $K = 15.27$, where the first one has the higher signal-to-noise ratio (∼8) of the two. This translates to $M_K = -26.45 \pm 0.1$ with the same *K*-correction and evolution correction as above. The second *K*-band determination would make the host one magnitude fainter. Either way, the host is found to be very bright also by using the surface brightness method in the *K*-band.

Experience with other elliptical galaxies in this brightness class (e.g. M87) has shown that if we restrict our measurements within 30 kpc distance from the centre, we are missing more than a negligible amount of light from the outer envelope of the galaxy. For example, the absolute *V*-magnitude of NGC 4889 (Sandage 1972)

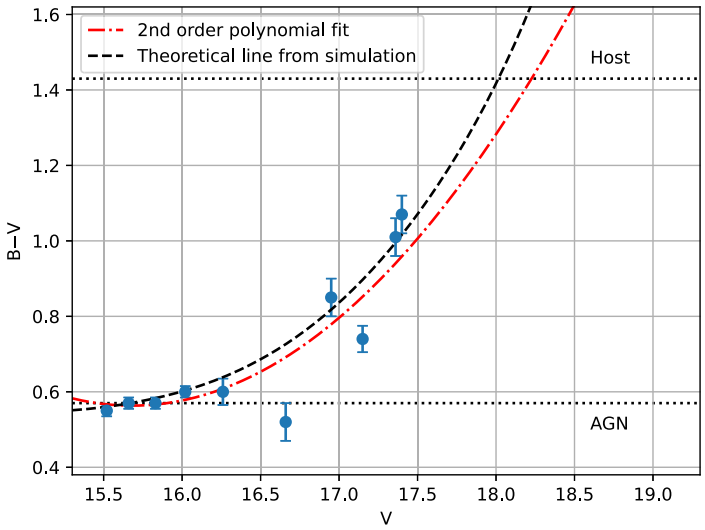

Figure 3. The variation of the $B - V$ colour as a function of V-band magnitude in OJ 287. The points above $V = 16.2$ refer to the 1989 fade, the others come from our Tables 1 and 2, and are averages of 10 measurements each. The red dash–dotted line represents a second-order polynomial fit to the data points. The black dashed line shows the expected colour index variation if a host of $V = 18.0$ is added to the AGN of constant colour. The horizontal dotted lines represent the expected host galaxy colour and the AGN colour, respectively.

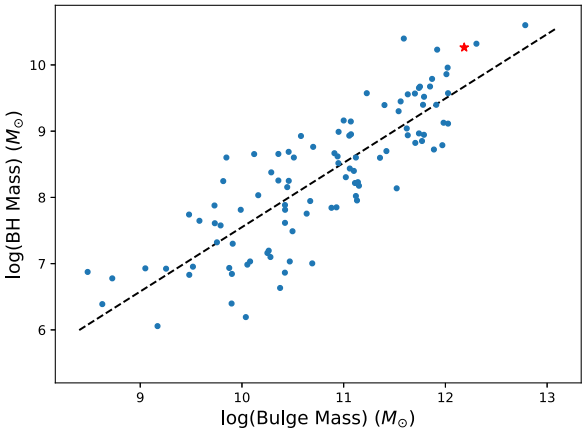

Figure 4. The galaxy sample of Saglia et al. (2016) in the BH mass versus galaxy stellar mass diagram (blue points), while the position of OJ 287 is given as a red star. OJ 287 is taken to be 0.3 mag fainter than NGC 4889. Three recent additional measurements have been added: NGC 1600 (Thomas et al. 2016), Abell 1201 central galaxy (Smith, Lucey & Edge 2017), and Holm 15A (Mehrgan et al. 2019). We note that OJ 287 lies within the 1σ scatter from the mean linear correlation (dashed line).

is $M_V = -22.2$ (using $m - M = 34.7$) measured out to roughly the same 30 kpc linear distance as the K-band data of Nilsson et al. (2020), while its total magnitude out to 100 kpc distance is about $M_V = -23.6$ (Graham & Scott 2013). Typically the outer envelope contributes about 0.8 mag to the total brightness (De Vaucouleurs & De Vaucouleurs 1970; Huang et al. 2013; Läsker, Ferrarese & van de Ven 2014).

The colour method measures all the light from the galaxy, including the outer envelope within the diaphragm of the photometer. In this case, it is roughly equivalent to 35 kpc linear distance at OJ 287. Therefore, some of the light of the host galaxy is missed by this method. In the imaging method, the outer envelope may be missed altogether if the data are not sufficient to include it in the model. In OJ 287, the point spread function of the central point source prevents the determination of the accurate sky background, necessary to measure the magnitude of the outermost component. Going towards shorter wavelengths, the signal-to-noise ratio becomes considerably worse due to the AGN component becoming more and more dominant. In the I-band, the signal-to-noise ratio falls below 5 (Nilsson et al. 2020), and at shorter wavelengths the situation becomes even worse. Probably for this reason, some other surface brightness measurements seem to have seriously underestimated the true brightness of the OJ 287 host galaxy (Wurtz, Stocke & Yee 1996; Heidt et al. 1999). The *Hubble Space Telescope* I-band measurement by Yanny, Jannuzi & Impey (1997), translated to K-band, gives the brightness upper limit at $M_K \sim -26.3$, in agreement with our result especially if the missing low brightness outer halo is taken into account.

Our magnitude determination is based on the assumption that the colour of OJ 287 at low light level is modified by the light of the host galaxy. It is also possible that there is a 'cosmic conspiracy', that is, the colour of OJ 287 evolves at low light levels because the AGN mimics the effects of the host. However, in this case, one might assume that the colour behaviour should be related to the relative flux decline, and we should see a similar behaviour in 2017 as in 1989 and 1999. On the other hand, if the colour changes are related to the absolute brightness levels, such as if the constant host galaxy is influencing the colours, then the 2017 fade should be quite different from the earlier deep fades. The latter has clearly been the case.

It appears that lowering the AGN activity does not in itself cause the observed colour changes. If indeed the base level brightness variation is due to the varying Doppler boosting (Valtonen & Pihajoki 2013), then the current 2017 fade is about as deep as the 1989–1999 fades in relative terms. The colour changes should be seen now as they were seen on earlier occasions. The three high-accuracy points from Krakow and Mt. Suhora Observatories during the last fade (see also the points on the left-hand side of Fig. 3) demonstrate that this is not the case.

Komossa et al. (2020, 2021a) confirm this result over a wider spectral range, using SEDs from the optical to ultraviolet (UV) (and X-rays as well), taken with the Neil Gehrels Swift observatory

Table 3. Summary of Swift observations.

V	$B-V$	$V/W2$
16.0	0.55 ± 0.03	1.47 ± 0.05
15.6	0.60 ± 0.03	1.58 ± 0.05
15.2	0.54 ± 0.03	1.49 ± 0.05
14.8	0.53 ± 0.03	1.46 ± 0.05

(Swift hereafter) at a cadence of 1–2 d in the course of the program MOMO (Multiwavelength observations and modelling of OJ 287; see Komossa et al. 2021b). All optical and UV bands, and the X-rays are near simultaneous, the UV–optical bands within minutes. In particular, Komossa et al. (2021a) reported that the ratio of UV flux over optical flux ratio is constant throughout the deep fade, and therefore excluded an extinction event, because the Swift UV bands are very sensitive to extinction. Table 3 gives the average $B-V$ colour and the V-band over UV-band W2 flux ratio at 4 brightness levels. It shows no significant colour trends with brightness. Going to the other direction on the wavelength axis, Kidger et al. (1998) have found that between infrared and optical regions, there are no colour changes over the V-magnitude range from 14.7 to 15.7.

The colour changes are apparently related to the absolute brightness of OJ 287. The influence of the host galaxy naturally explains this fact and seems to exclude the possibility that there is something in the jet emission mechanism that changes the colour depending on the blazar flux level.

It is likely that deep fades will happen in OJ 287 also in future. They will provide an excellent opportunity to probe the outer envelope of this galaxy further. There is no reason why the photometry during the fade should be limited only within 6 arcsec from the centre. While the direct imaging of the outer envelope is challenging, the separation of the host from the AGN by the colour method is rather simple. And on the basis of the excellent agreement of the magnitudes of the host galaxy by the two different methods we have demonstrated, the colour separation is a reliable method, and it could be recommended for the study of host galaxies in other AGN as well. The method is particularly well suited for the detection of low brightness level components of the host galaxies. Suitable candidates for such wide aperture photometry are found among the lowest redshift BL Lacertae objects (Urry et al. 2000). To our knowledge, such a study has never been attempted. It is understandable, since it takes a large amount of observing time to sample the BL Lacertae objects at different light levels, and moreover, the result cannot be deduced from usual photometry where the aperture is chosen so as to eliminate the influence of the host on the AGN magnitude.

The fades may arise from a temporary misalignment of the jet with regard to its average direction (Takalo et al. 1990). The jet appears to wiggle (Gomez et al. 2022) and in principle these wiggles are predictable (Dey et al. 2021). The modelling of the time behaviour of the optical polarization may be a way to predict also the optical fades. Alternatively, the fades may represent times of a change in accretion flow affecting (reducing) the jet emission, and it may also be possible to predict such moments of time (Valtonen et al. 2022).

ACKNOWLEDGEMENTS

We would like to thank Roberto Saglia for providing information on black hole mass measurements in advance of publication and for enlightening discussions. SZ would also like to acknowledge support of the NCN grant no. 2018/29/B/ST9/01793, and KM JSPS KAKENHI grant no. 19K03930.

DATA AVAILABILITY

The data published in this paper are available upon request from the authors.

REFERENCES

Bruzual A. G., 1983, ApJ, 273, 105
Chilingarian I. V., Melchior A.-L., Zolotukhin I. Y., 2010, MNRAS, 405, 1409
Ciprini S. et al., 2008, Proc. Sci., OJ 287 Colors During a Multifrequency Campaign. SISSA, Trieste, PoS(BLAZARS2008)030
De Vaucouleurs G., De Vaucouleurs A., 1970, Astrophys. Lett., 5, 219
Dey L. et al., 2018, ApJ, 866, 11
Dey L. et al., 2019, Universe, 5, 108
Dey L. et al., 2021, MNRAS, 503, 4400
Efimov Yu. S., Shakhovskoy N. M., Takalo L. O., Sillanpää A., 2002, A&A, 381, 408
Fioc M., Rocca-Volmerange B., 1997, A&A, 326, 950
Gómez J. L. et al., 2022, ApJ, 924, 122
Graham A., Scott N., 2013, ApJ, 764, 151
Guiderdoni B., Rocca-Volmerange B., 1987, A&A, 186, 1
Guiderdoni B., Rocca-Volmerange B., 1988, A&AS, 74, 185
Hagen-Thorn V. A. et al., 1998, A&AS, 133, 353
Heidt J. et al., 1999, A&A, 352, L11
Ho L. C., Li Z.-Y., Barth A. J., Seigar M. S., Peng C. Y., 2011, ApJS, 197, 21
Huang S., Ho L. C., Peng C. Y., Li Z.-Y., Barth A. J., 2013, ApJ, 766, 47
Kidger M. R. et al., 1995, A&AS, 113, 431
Kidger M. et al., 2018, A&A, 610, A74
Komossa S., Grupe D., Parker M. L., Valtonen M. J., Gómez J. L., Gopakumar A., Dey L., 2020, MNRAS, 498, L35
Komossa S. et al., 2021a, ApJ, 923, 51
Komossa S. et al., 2021b, Universe, 7, 261
Kristian J., Sandage A., Westphal J. A., 1978, ApJ, 221, 383
Läsker R., Ferrarese L., van de Ven G., 2014, ApJ, 780, 69
Lehto H. J., Valtonen M. J., 1996, ApJ, 460, 207
Massaro E. et al., 2003, A&A, 399, 33
Mehrgan K., Thomas J., Saglia R., Mazzalay X., Erwin P., Bender R., Kluge M., Fabricius M., 2019, ApJ, 887, 195
Nilsson K., Takalo L. O., Lehto H. J., Sillanpää A., 2010, A&A, 516, A60
Nilsson K. et al., 2020, ApJ, 904, 102
Padovani P., Giommi P., 1995, ApJ, 444, 567
Pietilä H. et al., 1999, A&A, 345, 760
Pihajoki P. et al., 2013, ApJ, 764, 5
Portinari L., Kotilainen J., Falomi R., Decarli R., 2012, MNRAS, 420, 732
Saglia R. P. et al., 2016, ApJ, 818, 47
Sandage A., 1972, ApJ, 176, 21
Sillanpää A., Haarala S., Valtonen M. J., Sundelius B., Byrd G. G., 1988, ApJ, 325, 628
Sitko M. L., Junkkarinen V. T., 1985, PASP, 97, 1158
Smith R. J., Lucey J. R., Edge A. C., 2017, MNRAS, 471, 383
Takalo L. O., Kidger M., de Diego J. A., Sillanpää A., Piirola V., Teräsranta H., 1990, A&AS, 83, 459
Thomas J., Ma C.-P., McConnell N. J., Greene J. E., Blakeslee J. P., Janish R., 2016, Nature, 532, 340
Urry C. M., Scarpa R., O'Dowd M., Falomo R., Pesce J. E., Treves A., 2000, ApJ, 532, 816
Valtonen M. J., Pihajoki P., 2013, A&A, 557, 28
Valtonen M. J. et al., 2006, ApJ, 646, 36
Valtonen M. J. et al., 2010, ApJ, 709, 725
Valtonen M. J., Ciprini S., Lehto H. J., 2012, MNRAS, 427, 77
Valtonen M. J. et al., 2016, ApJ, 819, L37
Valtonen M. J. et al., 2022, Galaxies, 10, 1
Wurtz R., Stocke J. T., Yee H. K. C., 1996, ApJS, 103, 109
Yanny B., Jannuzi B. T., Impey C., 1997, ApJ, 484, L113

[1]*Finnish Centre for Astronomy with ESO, University of Turku, Quantum, Vesilinnantie 5, FI-20014 Turun Yliopisto, Finland*
[2]*Tuorla Observatory, Department of Physics and Astronomy, University of Turku, Quantum, Vesilinnantie 5, FI-20014 Turun Yliopisto, Finland*
[3]*Department of Astronomy and Astrophysics, Tata Institute of Fundamental Research, Mumbai 400005, India*
[4]*Astronomical Observatory, Jagiellonian University, ul. Orla 171, PL-30-244 Krakow, Poland*
[5]*Mt Suhora Observatory, Pedagogical University, ul. Podchorazych 2, PL-30-084 Krakow, Poland*
[6]*Space Science Data Center - Agenzia Spaziale Italiana, via del Politecnico, snc, I-00133 Roma, Italy*
[7]*Instituto Nazionale di Fisica Nucleare, Sezione di Perugia, I-06123 Perugia, Italy*
[8]*European Space Agency European Space Astronomy Centre, E-28691 Villanueva de la Cañada, Madrid, Spain*
[9]*Nordic Optical Telescope, Apartado 474, E-38700 Santa Cruz de La Palma, Spain*
[10]*Astronomical Institute, Osaka Kyoiku University, 4-698 Asahigaoka, Kashiwara, Osaka 582-8582, Japan*
[11]*Dark Sky Observatory, Department of Physics and Astronomy, Appalachian State University, Boone, NC 28608, USA*
[12]*Max-Planck-Institut für Radioastronomie, Auf dem Hügel 69, D-53121 Bonn, Germany*
[13]*Physics Department, University of Perugia, via A. Pascoli, I-06123 Perugia, Italy*
[14]*Astronomical Observatory of Taras Shevshenko National University of Kyiv, Observatorna str 3, UA-04053 Kyiv, Ukraine*
[15]*Institute for Astronomy, Astrophysics, Space Applications and Remote Sensing, National Observatory of Athens, Metaxa & Vas. Pavlou St, Penteli, Athens GR-15236, Greece*
[16]*BAA Variable Star Section, West Challow Observatory, OX12 9TX Wantage, UK*
[17]*Instituto de Astrofísica de Andalucía (IAA-CSIC), P.O. Box 03004, E-18080 Granada, Spain*
[18]*Aritz Bidea No 8 4B (48100) Mungia Bizkaia, E-48100, Spain*
[19]*Muñas de Arriba La Vara, Valdés (MPC J38), E-33780 Valdés, Asturias, Spain*
[20]*Section of Astrophysics, Astronomy and Mechanics, Department of Physics, National and Kapodistrian University of Athens, GR-15784 Zografos, Athens, Greece*
[21]*ICAMER Observatory of NASU, 27, Acad. Zabolotnoho str, UA-03143 Kyiv, Ukraine*
[22]*Max Planck Institute for Astronomy, Koenigstuhl 17, D-69117 Heidelberg, Germany*
[23]*Dept. of Physics, Earth Science, and Space System Engineering, Morehead State University, 235 Martindale Dr, Morehead, KY 40351, USA*
[24]*Department of Physics and Astronomy, University of North Carolina at Chapel Hill, Chapel Hill, North Carolina NC 27599, USA*
[25]*16 Westminster Close Basingstoke Hampshire RG22 4PP, RG22 4PP Basingstoke, UK*
[26]*Department of Theoretical Physics and Astrophysics, Masaryk University, Kotlarska 2, CZ-61137 Brno, Czech Republic*
[27]*Department of Astronomy, The Ohio State University, 140 West 18th Avenue, Columbus, OH 43210, USA*
[28]*Center for Cosmology and Astroparticle Physics, The Ohio State University, 191 West Woodruff Avenue, Columbus, OH 43210, USA*
[29]*Astrophysikalisches Institut und Universitäts-Sternwarte, Schillergässchen 2-3, D-07745 Jena, Germany*
[30]*C/Jaume Balmes No 24, Cabrils, E-08348 Barcelona, Spain*
[31]*BAA Variable Star Section, 67 Ellerton Road, Kingstanding, Birmingham B44 0QE, UK*
[32]*Indian Institute of Astrophysics, II Block, Koramangala, Bengaluru 560034, India*
[33]*Astronomy and Space Physics Department, Taras Shevshenko National University of Kyiv, Volodymyrska str 60, UA-01033 Kyiv, Ukraine*
[34]*Konkoly Observatory, Research Centre for Astronomy and Earth Sciences, Eötvös Loránd Research Network (ELKH), Hungarian Academy of Sciences, Konkoly-Thege Miklós út 15–17, 1121 Budapest, Hungary*
[35]*C/Petrarca 6 1ª 41006 Sevilla, E-41006 Sevilla, Spain*
[36]*Faculty of Physics, Astrophysics and Astronomy Teaching Programme, Seville University, E-41004 Seville, Spain*
[37]*Department of Physics, University of Adiyaman, Adiyaman 02040, Turkey*
[38]*Astrophysics Application and Research Center, Adiyaman University, Adiyaman 02040, Turkey*
[39]*Florida International University and SARA Observatory, University Park Campus, Miami, FL 33199, USA*
[40]*Institute of Astronomy, Faculty of Physics, Astronomy and Informatics, Nicolaus Copernicus University in Toruń, ul. Grudziądzka 5, PL-87-100 Toruń, Poland*

This paper has been typeset from a TEX/LATEX file prepared by the author.